Article

Hsc70 is required for endocytosis and clathrin function in *Drosophila*

Henry C. Chang,[1] Sherri L. Newmyer,[2] Michael J. Hull,[1] Melanie Ebersold,[1] Sandra L. Schmid,[2] and Ira Mellman[1]

[1]Department of Cell Biology, Ludwig Institute for Cancer Research, Yale University School of Medicine, New Haven, CT 06520
[2]Department of Cell Biology, Scripps Research Institute, La Jolla, CA 92037

By screening for *Drosophila* mutants exhibiting aberrant bride of sevenless (Boss) staining patterns on eye imaginal disc epithelia, we have recovered a point mutation in *Hsc70-4*, the closest homologue to bovine clathrin uncoating ATPase. Although the mutant allele was lethal, analysis of mutant clones generated by *FLP/FRT* recombination demonstrated that the Sevenless-mediated internalization of Boss was blocked in mutant *Hsc70-4* eye disc epithelial cells. Endocytosis of other probes was also greatly inhibited in larval Garland cells. Immunostaining and EM analysis of the mutant cells revealed disruptions in the organization of endosomal/lysosomal compartments, including a substantial reduction in the number of clathrin-coated structures in Garland cells. The *Hsc70-4* mutation also interacted genetically with a dominant-negative mutant of dynamin, a gene required for the budding of clathrin-coated vesicles (CCVs). Consistent with these phenotypes, recombinant mutant Hsc70 proteins exhibited diminished clathrin uncoating activity in vitro. Together, these data provide genetic support for the long-suspected role of Hsc70 in clathrin-mediated endocytosis, at least in part by inhibiting the uncoating of CCVs.

Introduction

Endocytosis, a process common to all eukaryotic cells, plays a critical role not only in the internalization of extracellular macromolecules but also in the down-regulation of signaling receptors from the cell surface. One major route of endocytosis is the clathrin-mediated pathway, characterized by the selective internalization of receptors and bound ligands via clathrin-coated vesicles (CCVs).* To facilitate multiple rounds of endocytosis, it has long been appreciated that the clathrin coats must be dissociated from CCVs soon after vesicle formation and reutilized for subsequent rounds of endocytosis. At least in vitro, clathrin uncoating activity has been associated with the Hsc70 ATPase and its accessory protein, auxilin (Schlossman et al., 1984; Chappell et al., 1986; Ungewickell et al., 1995).

Hsc70 is a constitutively expressed member of the Hsp70 protein family that has been implicated in many processes including folding of newly synthesized polypeptides, trans-location of proteins across the endoplasmic reticulum, stabilizing proteins under stress conditions, and antigen presentation (Bukau and Horwich, 1998). In vitro, Hsc70 promotes the release of clathrin triskelions and other coat proteins from CCVs by binding to clathrin and thus disrupting the clathrin cage concomitant with ATP hydrolysis (Schlossman et al., 1984; Hannan et al., 1998). Like other members of the Hsp70 protein family, Hsc70 has a low intrinsic ATPase activity, which can be stimulated by cofactors (Ungewickell et al., 1995; Bukau and Horwich, 1998). The relevant cofactor in the uncoating reaction is thought to be auxilin, a member of the DnaJ protein family characterized by a conserved J-domain motif (Ungewickell et al., 1995; Umeda et al., 2000). In addition, auxilin contains a clathrin binding domain, suggesting that auxilin first binds to CCVs, and then recruits ATP-bound Hsc70 proteins via its J-domain (Ungewickell et al., 1995; Holstein et al., 1996). The J-domain interaction stimulates Hsc70 ATPase activity, thereby stabilizing the binding of Hsc70 to clathrin, and driving triskelion dissociation (Holstein et al., 1996). After uncoating, Hsc70 remains associated with the soluble pool of clathrin (Schlossman et al., 1984).

Despite these advances in understanding the mechanism of Hsc70-mediated clathrin uncoating in vitro, its role in vivo is less clear. Certainly, Hsc70 has diverse functions, making a selective analysis of its effects on endocytosis difficult. Further complicating matters is the fact that Hsc70 is an abundant protein. Indeed, defects in the endocytic pathway

were not detected in a partial loss of function *Drosophila Hsc70* mutant (Bronk et al., 2001). Thus far, the only evidence that Hsc70 has a role in endocytosis comes from experiments involving the introduction of high concentrations of Hsc70 inhibitory antibodies, peptides, or dominant interfering mutants, conditions which disrupt the internalization and recycling of membrane receptors and neurotransmitters (Honing et al., 1994; Morgan et al., 2001; Newmyer and Schmid, 2001). Although these results are consistent with the biochemical properties of Hsc70 as the uncoating ATPase, the role of Hsc70 in endocytosis under physiological conditions has yet to be demonstrated.

We have taken an unbiased genetic approach to identify genes required for endocytosis and cell polarity using *Drosophila* eye imaginal discs. The developing eye was chosen for two reasons: (1) there is a convenient technology, the *FLP/FRT* recombination system (Xu and Rubin, 1993), that facilitates the production of mutant tissues of potentially lethal genes at a high efficiency; and (2) there is a convenient marker, *bride of sevenless* (*boss*) (Cagan et al., 1992), that permits a simple assay for polarized endocytosis at the apical surface of eye disc epithelial cells.

The *Drosophila* eye is comprised of regular arrays of ~800 repeated units called ommatidia. Each ommatidium contains eight photoreceptors (R1–R8) that are sequentially recruited from undifferentiated epithelial cells in the eye imaginal discs during larval development. One of the best-understood events in this complex process is the determination of the R7 photoreceptor cell fate, which requires the *sevenless* (*sev*) receptor tyrosine kinase and *boss*, a seven transmembrane ligand for Sev (Zipursky and Rubin, 1994). Although *boss* and *sev* are both required for specifying the R7 cell fate, they function in different cells. Boss proteins are only expressed on the apical surface of the R8 cells, whereas Sev proteins are expressed on the apical surface of the R3, R4, R7, and cone cell precursors (Tomlinson et al., 1987; Hart et al., 1990). Interestingly, upon binding to Sev, the Boss proteins, including the cytoplasmic portions, are internalized into an endosomal structure in the Sev-expressing cells (Cagan et al., 1992). Although little is known about the machinery required for this receptor-mediated internalization, the internalization of Boss requires a dynamin-dependent pathway (Cagan et al., 1992). Here we describe the characterization of one mutant that affects a gene likely to participate in clathrin-mediated endocytosis.

Results

### *HS1-25* exhibits defects in membrane protein internalization in eye imaginal discs

The localization of Boss proteins can be easily monitored using a functional HRP–Boss chimera, in which the cytochemically detectable enzyme HRP was fused to the extracellular domain of Boss (Sunio et al., 1999). In wild-type eye discs, the staining pattern of HRP–Boss fusion is seen as "patches," representing Boss proteins on the apical surface of R8 cells, and "dots," representing those accumulated in structures in Sev-expressing cells (Cagan et al., 1992). Thus, the simplest strategy for identifying mutations defective for Boss trafficking would be to perform a traditional F₂ screen and examine the pattern of HRP–Boss staining in homozy-

gous mutant progeny. However, genes functioning in Boss trafficking might also be important for the trafficking of essential genes required early in embryogenesis; thus, mutations in these genes would likely cause death before eye development. To circumvent this problem, we examined the pattern of HRP–Boss staining in mutant clones generated by the *FLP/FRT* recombination system (Xu and Rubin, 1993). To this end, we constructed a series of *ey-FLP; HRP-Boss; FRT, arm-LacZ* fly lines that allow us to visualize Boss localization in mutant clones by simple DAB and X-gal reactions (see Materials and methods).

As an initial test of this strategy, we screened 1,032 mutagenized third chromosome right arms and isolated several mutants exhibiting aberrant HRP–Boss staining. One mutant, designated *HS1-25* (HRP–Boss screen) appeared to be the best candidate for a mutant defective in Boss trafficking. Fig. 1 A shows an example of an eye disc showing wild-type, heterozygote, and homozygote mutant tissue, indicated by decreasing intensities of blue β-galactosidase reaction product. In wild-type (+/+) and heterozygous (+/−) tissue, typical HRP–Boss staining was observed, i.e., a large patch corresponding to the central R8 cell (asterisks) surrounded by smaller dots representing HRP–Boss that had been internalized to endosomes of adjacent cells (arrowheads). In homozygous mutant tissue (−/−), however, only the central HRP–Boss patch was observed, suggesting that Boss had not been properly internalized.

As we suspected, the *HS1-25* mutation was recessive lethal, although some rare homozygotes did survive until the larval stage. These homozygous *HS1-25* larvae were thinner, more translucent, and developmentally delayed compared with wild type. Furthermore, they often contained melanotic masses (~20%) and cell clumps near their brains (~100%). Despite some disorganization and delays in ommatidial assembly (unpublished data), the eye discs dissected from homozygous third instar mutant larvae exhibited the same patterns of Boss staining as were found in the *FLP/FRT*-induced mutant clones (Fig. 1 B). The Boss staining in the mutant eye discs was entirely distinct from discs harvested from wild-type larvae at the same stage (Fig. 1 C).

Because the internalization of Boss requires Sev receptors, one possible explanation for the mutant phenotype is that Sev receptors were not expressed or localized properly to the apical surface in *HS1-25* eye discs. We thus examined the expression and localization of Sev receptors in *HS1-25* mutant tissues generated by *FLP/FRT* recombination. To facilitate the identification of homozygous mutant cells, wild-type and heterozygous cells were labeled with a myristoylated, membrane-associated GFP (see Materials and methods for details). As mentioned above, Sev receptors are expressed on the apical surface of R3, R4, R7, and cone cell precursors in wild-type eye discs (Fig. 1, D–F; Tomlinson et al., 1987). In *HS1-25* mutant cells, Sev receptors were still expressed and localized to the apical surfaces (Fig. 1, D–F). Thus, the defect in Boss internalization was not due to a mislocalization or absence of Sev expression resulting in a failure of receptor–ligand interaction. This conclusion was further supported by the observation that the mutant R7 cells were specified normally, as shown in tangential sections of *HS1-25* adult retina clones (Fig. 1 G, R7 cells indicated by arrowheads), indicating that
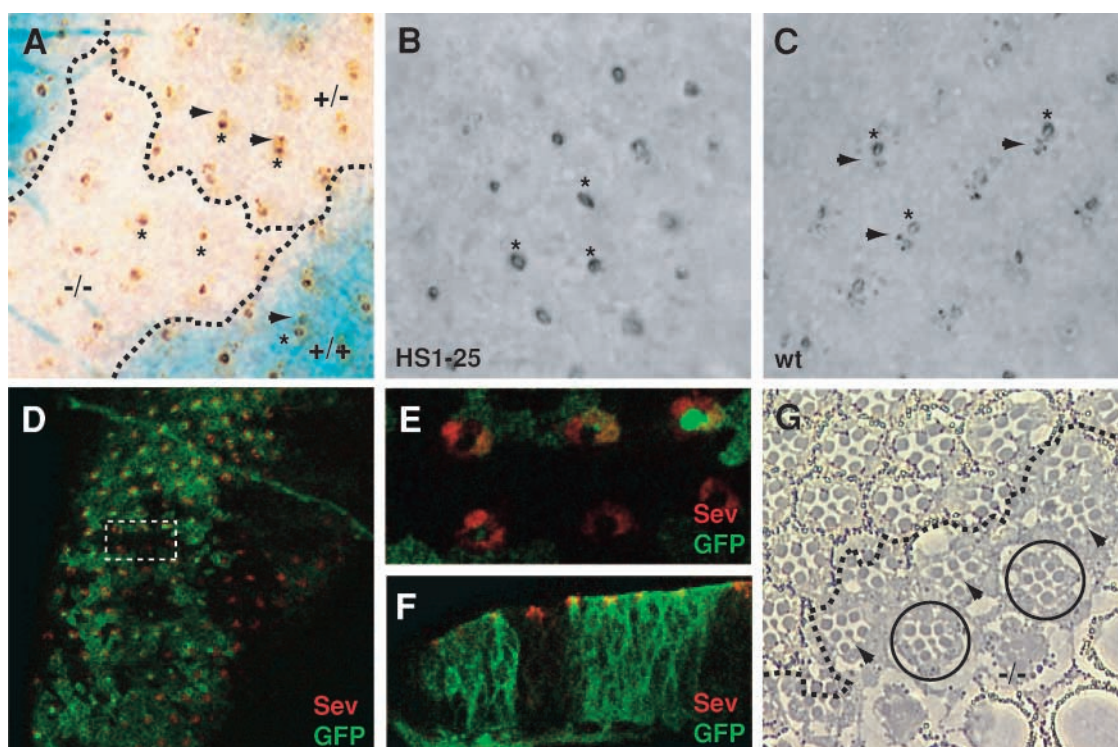
Figure 1. **HS1-25 is defective for Boss internalization.** (A) A clone of *HS1-25* in a third instar eye imaginal disc. The genotypes for most of the cells in this eye disc are heterozygous for *HS1-25* (marked as +/−), represented by the heterozygous lacZ region (light blue). Cells homozygous for *HS1-25* are located in the lacZ-negative patch (white). The "twin spot," where homozygous wild-type cells are located, is homozygous lacZ positive (dark blue). The Boss proteins on the apical surface of R8 cells are labeled by asterisks, and the Boss internalized by the neighboring cells is indicated by arrowheads. Dash lines delineate the boundaries between regions of various genotypes. (B and C) Third instar *HS1-25* (B) and wild-type (C) eye imaginal discs carrying HRP–Boss. The Boss proteins on the apical surface of R8 cells are labeled by asterisks, and the Boss internalized by the neighboring cells is indicated by arrowheads. Note that the accumulations of Boss in neighboring cells are absent in B. (D–F) Confocal images of a mosaic third instar eye imaginal disc stained with a mouse αSev antibody (Texas red). Wild-type cells are indicated by the presence of a membrane-associated GFP expression, whereas mutant cells are indicated by the absence of GFP expression. (D) A confocal planar section of *HS1-25* clones in a mosaic eye disc. Because this section plane is near the apical surface of the cells, the GFP staining has a smooth appearance, instead of the honeycomb-like appearance observed in lower focal planes (see Fig. 3 H). The rectangular area is shown in a higher magnification in E. (F) A cross section of an *HS1-25* clone in a mosaic eye disc. (G) A tangential section an *HS1-25* clone in adult retina. Mutant photoreceptor cells are represented by those lacking white pigment granules at the base of their rhabdomeres, and delineated by the dash line. Mutant R7 cells are indicated by arrowheads. Normal clusters comprised entirely of mutant cells are indicated by circles.

Sev and Boss were still functioning properly at the cell surface. A disruption of the Sev–Boss interaction by *HS1-25* would most likely have caused the classical "R7-less" phenotype.

Although the phenotype of *HS1-25* suggested a defect in membrane protein internalization, the mutation had little effect on photoreceptor differentiation. Only occasional ommatidial clusters exhibited missing photoreceptors. For the most part, even clusters comprised of entirely mutant cells were able to differentiate and assemble normally (Fig. 1 G, clusters indicated by circles).

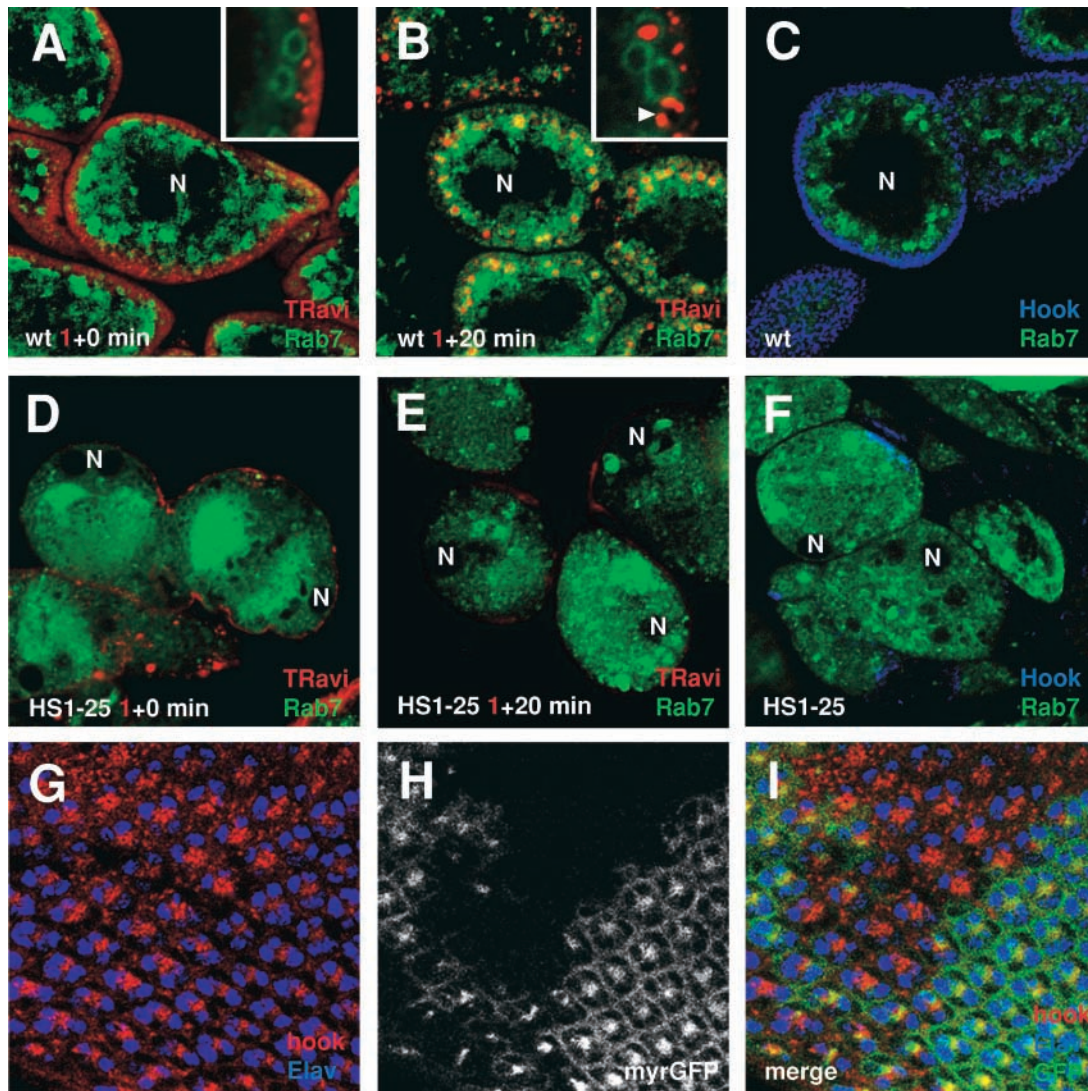## Uptake of an endocytic tracer and endosomal organization are disrupted in *HS1-25* Garland cells

To test whether *HS1-25* has more generalized endocytic defects in other tissues, we examined the effect of *HS1-25* on the uptake of an endocytic tracer, Texas red–conjugated avidin (TR-avidin), by Garland cells isolated from mutant larvae. Garland cells are thought to function as nephrocytes and have a rapid rate of fluid phase endocytosis (Kosaka and Ikeda, 1983). After 1 min at 25°C, internalized TR-avidin could be

seen in peripheral vesicular structures in wild-type Garland cells (Fig. 2 A). To help characterize this compartment, these cells also carried an *Act5C-GAL4; UAS-GFP-rab7* transgene (Entchev et al., 2000), which mostly labels late endosomes. As shown in Fig. 2 A, most of the TR-avidin–positive structures were peripherally localized as compared with the Rab7-positive late endosomes. This was particularly evident in the high magnification confocal image shown in the inset.

In contrast, after a 20-min chase, most of the TR-avidin was found within the Rab7-positive structures, suggesting that the tracers were in late endosomes or lysosomes (Fig. 2 B, inset). Interestingly, the TR-avidin often appeared as distinct punctate structures contained inside larger Rab7-positive vacuoles (Fig. 2 B, inset, arrowhead). Although possibly representative of aggregated TR-avidin, we suspect that the tracer actually labeled internal multivesicular elements known to be present in late endocytic compartments (Fergestad et al., 1999).

Importantly, no vesicular staining of TR-avidin was seen in *HS1-25* Garland cells either after 1 min of uptake (Fig. 2

Figure 2.   ***HS1-25* Garland cells are defective in endocytic tracer uptake, and exhibit disorganized endosomal/lysosomal compartments.**
Uptake of TR-avidin by wild-type (A and B) and *HS1-25* (D and E) Garland cells. Cells were incubated in M3 media containing TR-avidin for 1
min and chased for 0 min (A and D) and 20 min (B and E). The cells also expressed a GFP–Rab7 fusion to identify late structures in the endocytic
pathway. For the sake of consistency, all confocal images of Garland cells shown are those cross sections near the plane of their nuclei (N).
Note that these cells are dinucleate. High magnification images of the cell periphery are shown in insets of A and B. A Rab7-positive structure
with multiple punctate staining of TR-avidin is indicated with an arrowhead. (C and F) Third instar wild-type (C) and *HS1-25* (F) larval Garland
cells were stained with a rabbit αHk antibody (Cy5). As in the uptake assay, these cells also carried the GFP–Rab7 transgene. (G–I) Confocal
images of *HS1-25* clones in a mosaic eye disc. (G) The cells were stained with a rabbit αHk antibody (Texas red) and a rat αElav antibody (Cy5)
to label early endocytic structures and nuclei of neuronal cells, respectively. (H) Wild-type cells are indicated by the presence of a membrane-
associated GFP expression, whereas mutant cells are indicated by the absence of GFP expression. (I) A merged image of G and H.

D) or after a chase of 20 min (Fig. 2 E). This indicates that
the internalization of endocytic tracers was completely
blocked in mutant cells.

Given that the uptake of the endocytic tracers into Rab7-
positive late endosomes was strongly inhibited, we tested
whether *HS1-25* had defects in endosomal organization by
comparing the staining pattern of Hook (Hk), a cytosolic
protein associated with early endosomes (Kramer and Phis-
try, 1996), and GFP–Rab7 in both wild-type and *HS1-25*
mutant tissues. In wild-type Garland cells, Hk was associated
with structures located around the cell periphery in the same
region where the 1-min TR-avidin pulse was localized and
spatially distinct from the bulk of the Rab7 staining (Fig. 2

C). In contrast, Hk staining was patchy and greatly reduced
in *HS1-25* Garland cells (Fig. 2 F). In addition, Rab7 ap-
peared more diffuse and centrally located in *HS1-25* Garland
cells (Fig. 2, D–F). Although the ring-like Rab7-positive
structures were still present in *HS1-25* cells, the morphology
and amount of Rab7 associated seemed to vary noticeably.

A defect in Hk localization was also detected in mosaic eye
imaginal discs generated by FLP/FRT recombination (Fig.
2, G–I). To identify the cell clusters, the eye discs were also
stained with an αElav antibody, which labels the nuclei of
neuronal cells (Robinow and White, 1988). In wild-type
cells (indicated by the presence of GFP expression), Hk was
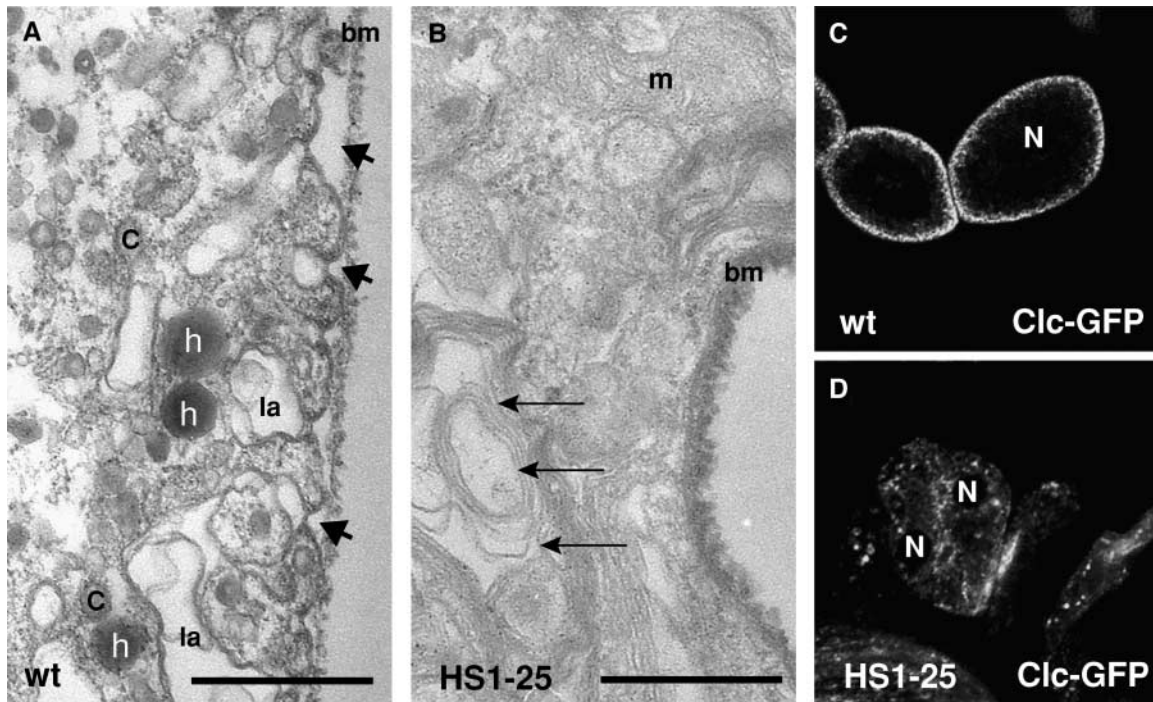concentrated near the apical cortex of photoreceptor cells. In

Figure 3. **HS1-25 Garland cells have a reduced number of clathrin-coated structures.** Transmission electron micrographs of wild-type (A) and *HS1-25* (B) Garland cells. These cells were subjected to HRP uptake for 5 min, fixed, and processed for EM analysis. In A, arrows indicate HRP-positive vesicles, and arrowheads indicate the opening of labyrinthine channels. C, coated vesicles; la, labyrinthine channel; bm, basement membrane; m, mitochondria. In B, arrows indicate the multilaminar lysosomal-like structures. Bars, 0.5 μm. (C and D) Confocal images of the wild-type (C) and *HS1-25* (D) larval Garland cells expressing a *Clc* GFP fusion.

HS1-25 mutant cells (indicated by the absence of GFP expression), the staining of Hk proteins appeared more vesicular, less restricted to the apical surface, and could be easily detected at lower focal planes of cells. Together these data suggest that the organization of endosomal compartments was affected by *HS1-25* mutation.

HS1-25 mutant cells contain a reduced number of CCVs

To better characterize the defects of *HS1-25*, we performed EM analysis on wild-type and *HS1-25* larval Garland cells. Isolated Garland cells were incubated for 5 min with HRP as an endocytic tracer, fixed, and then processed for EM (Kosaka and Ikeda, 1983). Similar to TR-avidin labeling, HRP-positive vesicles were readily identified in wild-type Garland cells (Fig. 3 A, labeled by "h"). In contrast, almost no HRP-positive vesicles were present in *HS1-25* mutant cells (Fig. 3 B). Some of the HRP appeared to accumulate on the surface of *HS1-25* cells instead.

In addition to the difference in the amount of HRP internalized, there were also dramatic morphological changes in *HS1-25* cells. The periphery of wild-type Garland cells are characterized by distinctive "labyrinthine channels," long invaginations extending from the cell membrane (∼3/μm) (Fig. 3 A, arrowheads). These channels are thought to be specialized endocytic intermediates, as they accumulate at the nonpermissive temperature in *shibire^{ts}* (*shi^{ts}*) Garland cells (Kosaka and Ikeda, 1983). In contrast, the labyrinthine channels were absent in mutant cells (Fig. 3 B). Furthermore, there was a complete absence of coated structures in mutant cells; in wild-type cells, coated vesicles were strikingly abun-

dant (Fig. 3 A, labeled by "C"). This phenotype demonstrates that endocytosis and clathrin function are greatly perturbed in the mutant cells and that the block in endocytosis precedes the shibire-dependent step. Finally, compared with wild-type cells, there was a dramatic increase of multilaminar lysosomal structures in mutant cells (Fig. 3 B, arrows), suggesting a defect in lysosomal function. Such a defect might also reflect an alteration in coated vesicle function, because clathrin is required not only for transporting internalized material to lysosomes but also for the delivery of lysosomal hydrolases (Schulze-Lohoff et al., 1985; Kornfeld and Mellman, 1989; Meyer et al., 2000; Puertollano et al., 2001).

To monitor the localization of clathrin more closely, we have constructed and expressed a *UAS-GFP–clathrin light chain* (*Clc*; CG6948) transgene in Garland cells using *Act5C-GAL4* driver lines. Previous studies demonstrated Clc–GFP to incorporate functionally into clathrin-coated pits that assemble at the cell surface (Gaidarov et al., 1999). In wild-type Garland cells, Clc labeling was seen as vesicular structures near the cell periphery, presumably representing CCVs (Fig. 3 C). In contrast, this vesicular pattern of Clc was greatly reduced and became more centrally located in *HS1-25* cells (Fig. 3 D). These results, together with the EM analysis, suggested that clathrin function was compromised by the *HS1-25* mutation.

HS1-25 interacts genetically with a gene in the clathrin-dependent pathway

Given the effects on endocytosis and the disruption of clathrin distribution observed in *HS1-25* cells, we suspected that
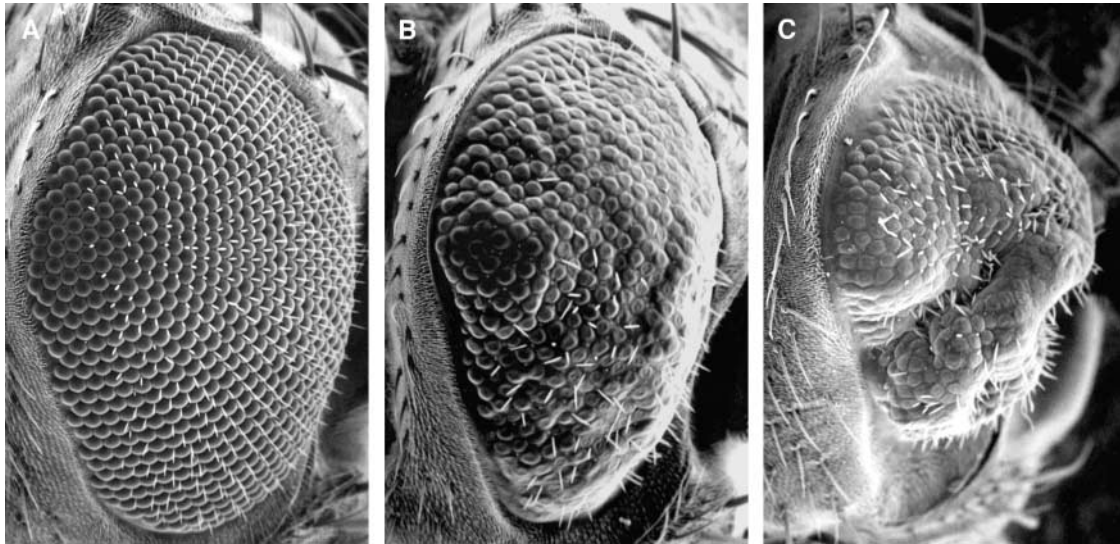
Figure 4. **HS1-25 interacts genetically with dynamin.** SEM of adult eyes of (A) *GMR-shi/+*, (B) *GMR-shi^{K39A}/+*, and (C) *GMR-shi^{K39A}/HS1-25*.

HS1-25 would interact with genes functioning in the clathrin pathway. To test this possibility, we used a fly line expressing a dominant negative allele of dynamin/*shi* under the control of an eye-specific promoter (*GMR-shi^{K39A}*) (van der Bliek and Meyerowitz, 1991; Hay et al., 1994). Dynamin is a GTPase involved in the physical budding of vesicles from the plasma membrane (Hinshaw, 2000). Although it is not yet clear if dynamin acts as a mechano-enzyme or also as a signaling molecule, loss of dynamin function clearly inhibits endocytosis (Sever et al., 2000). Furthermore, overexpression of a GTP hydrolysis–defective mutant dynamin can block transferrin uptake and recycling in HeLa cells (Damke et al., 1995, 2001). Expression of GTP hydrolysis–defective *Drosophila* dynamin (*shi^{K39A}*) using the *glass* expression cassette can partially inhibit Boss internalization in the eye discs (unpublished data). The incompleteness of this inhibition was likely due to an insufficient level of Shi^{K39A} expression.

Although overexpression of the wild-type dynamin has no effect on eye organization (Fig. 4 A), the *GMR-shi^{K39A}* construct caused a rough eye phenotype (Fig. 4 B), presumably due to an alteration in signaling caused by the inhibition of endocytosis. We thus crossed *HS1-25* to *GMR-shi^{K39A}* flies to test if *HS1-25* would synergize with *GMR-shi^{K39A}*. Although eyes heterozygous for *HS1-25* were completely normal, one copy of *HS1-25* enhanced the *GMR-shi^{K39A}*–induced rough eye phenotype (Fig. 4 C), suggesting that *HS1-25* functions on the dynamin-mediated pathway.

### HS1-25 is a mutation in the *Drosophila Hsc70-4* gene

To clone *HS1-25*, we first mapped the lethality of *HS1-25* by meiotic recombination to 3–57, between *cu* and *sr*. Although we were unable to find a deletion that uncovered the lethality of *HS1-25*, the mutation was tentatively placed in the cytological interval between 88E5 and 88E13, a small gap not covered by the deletions tested. Lethal complementation tests with genes in this region showed that *HS1-25* is an allele of *Hsc70-4*, as *HS1-25* failed to complement existing *Hsc70-4* alleles (*Hsc70-4^{L03929}*, *Hsc70-4^{P03550}*, and *Hsc70-4^{E195}*) (Hing et al., 1999). By sequence similarity, *Hsc70-4*

appears to be the *Drosophila* homologue of clathrin-uncoating ATPase (80% identity to bovine Hsc70; Perkins et al., 1990). Sequencing of genomic DNA isolated from *HS1-25* flies revealed a single amino acid change at Arg447 to His (R447H) in *Hsc70-4*. Furthermore, *Hsc70-4^{R447}* appeared to be the only lethal mutation in *HS1-25* flies because a genomic DNA fragment (Hing et al., 1999) carrying a wild-type *Hsc70-4* locus can rescue this lethality (unpublished data). *Hsc70-4^{R447H}* is likely to be a partial loss of function mutation, because homozygous *Hsc70-4^{R447H}* animals died later than *Hsc70-4* nulls (Bronk et al., 2001). In support of this possibility, *FLP/FRT* recombination failed to generate detectable mutant clones using null alleles of *Hsc70-4* (unpublished data).

Hsc70-4 is required for endocytosis and not polarized expression of Boss

In addition to endocytosis, CCVs are thought to transport cargo between the TGN and early endosomes (Kornfeld and Mellman, 1989). Furthermore, *Drosophila Hsc70-4* has been shown to cooperate with the cysteine string protein in synaptic exocytosis (Bronk et al., 2001). Thus, it was possible that the HRP–Boss endocytosis defect observed in the *HS1-25* mutant might reflect a block in the delivery of HRP–Boss to the apical surface of R8 cells; if the ligand did not make it to the apical surface, then it would not be available for endocytosis by *sev* receptors on adjacent R3, R4, or R7 cells. To determine if HRP–Boss had been properly delivered to the plasma membrane, we first asked if it was accessible to the membrane-impermeant reducing agent MESNA, which, like ascorbic acid, irreversibly reduces and inactivates HRP.

Wild-type and mutant eye discs carrying the HRP–Boss transgene were incubated in ice-cold 25 mM MESNA, pH 8.5, for 30 min, and then HRP activity was developed using DAB. In wild-type eye discs (Fig. 5 A), no reaction product was associated with R8 cells, indicating that the HRP activity had been completely accessible to inactivation by MESNA (compare with non-MESNA–treated wild-type eye discs in Fig. 1 C). The only HRP activity detected was found within
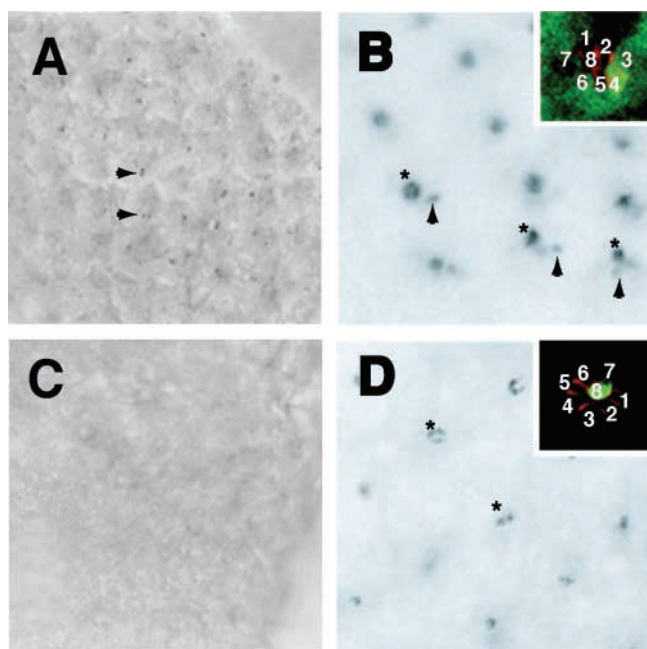
Figure 5.   *Hsc70-4* mutation affects the internalization of Boss by the Sev-expressing cells. Wild-type (A) and Hsc70 mutant (C) eye discs carrying HRP–Boss were treated with ice-cold MESNA and stained for HRP activities. The Boss internalized by the neighboring cells is indicated by arrowheads. (B and D) UAS-myc::Hsc70^wt^ were driven using sev-GAL4 (B) and sca-GAL4 (D) drivers in homozygous Hsc70 mutant eye discs. In the insets, one individual cluster was labeled with αMyc (FITC) and αArm (Texas red) to visualize Hsc70 expression and photoreceptor cell boundaries, respectively. (B and D) DAB staining third instar larval discs dissected from (B) *sev-Gal4/+, UAS-myc::Hsc4, hsc^R447H^/hsc^R447H^* and (D) *sca-Gal4/+, UAS-myc::Hsc4, hsc^R447H^/hsc^R447H^* animals. The Boss proteins on the apical surface of R8 cells are labeled by asterisks, and the Boss internalized by the neighboring cells is indicated by arrowheads.

R3, R4, and R7 cells, which had internalized HRP–Boss before MESNA treatment (Fig. 5 A, arrowheads). In *HS1-25* R8 cells, the HRP–Boss was also completely quenched by the MESNA treatment (Fig. 5 C), indicating that even in the mutant cells, the HRP–Boss fusion had reached the cell surface. Note that, as expected, no HRP–Boss staining was observed in the mutant R3, R4, or R7 cells due to the endocytosis defect. The inactivation of HRP–Boss by externally added MESNA in both wild-type and mutant R8 cells demonstrated that the *HS1-25* mutation did not block delivery of HRP–Boss to the R8 cell surface.

To demonstrate directly that the effect of the *HS1-25* mutation was due to inhibition of HRP–Boss internalization in the sev-expressing cells and not due to a defect in the secretory pathway in Boss-expressing cells, we used cell-specific *GAL4* drivers to selectively express a myc-tagged wild-type Hsc70-4 in either Boss-expressing (R8) or Boss-internalizing (R3, R4, and R7) cells (Brand and Perrimon, 1993). Antibody to Armadillo (β-catenin; red) was used to delineate the margins of individual photoreceptor cells (Peifer and Wieschaus, 1990). When expressed under the control of a *sev-GAL4* driver (Richardson et al., 1995), myc::Hsc70-4 (green) was expressed only in those cells (i.e., R3, R4, and R7) that internalize Boss, but not in R8 cells (Fig. 5 B, inset). Expression in homozygous *HS1-25* mutant eye discs

partially restored Boss endocytosis (Fig. 5 B, arrowheads, asterisks indicate HRP–Boss-expressing R8 cells). The incomplete rescue of the mutant phenotype was likely due to the insufficient expression of Hsc70-4 protein, which is normally very abundant (Perkins et al., 1990). In contrast, when *sca-GAL4^109–68^* driver (White and Jarman, 2000), active specifically in R8 cells (Fig. 5 D, inset), was used to express wild-type Hsc70-4, the internalization of Boss remained inhibited (Fig. 5 D). Together, these data demonstrate that the observed phenotype was caused by defects in the Boss-internalizing cells.

Hsc70^R447H^ has impaired clathrin uncoating activity in vitro

Hsp70 family proteins can be divided into three structural domains: the highly conserved NH$_2$-terminal ATPase domain; the substrate binding domain (SBD); and the less conserved carboxy-terminal domain. Situated in the SBD, the highly conserved Arg447 has been implicated as an important residue for forming a salt bridge with E521 (Morshauser et al., 1999). Thus the R447H substitution seemed likely to affect the conformation or substrate binding activity of Hsc70-4. To assay for possible alterations in conformation, the R447H mutation was generated in bovine Hsc70, and recombinant wild-type and mutant proteins were purified and subjected to proteolytic cleavage by endoproteinase LysC (LysC) in the presence of ATP or ADP. Compared with Hsc70^WT^, Hsc70^R447H^ exhibited more susceptibility to LysC in the presence of both nucleotides (Fig. 6 A, compare density of the ∼44-kD species). In addition, a somewhat different banding pattern was obtained for the mutant protein in the presence of ADP. Together, these data indicate conformational differences between wild-type and mutant Hsc70.

Because the SBD is required for Hsc70's interaction with clathrin triskelions (Chappell et al., 1987) and possibly with the accessory factor auxilin (Mayer et al., 1999), it seemed likely that the binding of Hsc70 to CCVs or auxilin might be affected by the R447H substitution. To test whether the binding of Hsc70 to CCVs was affected by the mutation, recombinant Hsc70 was added to CCVs, pelleted, and then subjected to SDS-PAGE analysis. As shown in Fig. 6 B, a similar amount of mutant Hsc70 was bound to CCVs as the wild type, suggesting that Hsc70^R447H^ retained the ability to bind to CCVs. To test whether the mutant proteins could still bind auxilin, wild-type and mutant recombinant proteins were subjected to GST pull-down assay using a GST–J^aux^ bait fusion (Holstein et al., 1996). As shown in Fig. 6 C, wild-type and mutant proteins both bound to the J-domain in the presence of ATP but not in the presence of ADP. No binding was seen with GST alone. These data suggested that the binding of Hsc70^R447H^ to auxilin was also not affected. Consistent with this, overexpression of *Drosophila auxilin* (CG1107) under the control of the *GMR* expression cassette in homozygous *HS1-25* could not compensate for the defects in HRP–Boss internalization (unpublished data).

Although no apparent differences in Hsc70 binding to CCVs and auxilin were observed, clathrin uncoating activity might still be compromised by the R447H mutation. This was determined by assaying the abilities of recombinant wild-

Figure 6. **Hsc70^{R447H} has a diminished clathrin uncoating activity.** (A) The nucleotide-dependent conformational change of the wild-type and mutant hsc70 proteins was detected by limited proteolysis in the presence of endoproteinase Lys C and 2 mM of the designated nucleotide. The 70-kD intact polypeptide and the 60- and 44-kD LysC cleavage products are indicated. (B) Wild-type and mutant hsc70 cosediment with CCVs. CCVs were sedimented and analyzed by SDS-PAGE. Background ~70-kD protein associated with the isolated CCVs is shown in the right lane. CHC, clathrin heavy chain. (C) Wild-type and mutant hsc70 bind the J-domain of auxilin. Hsc70 proteins were incubated with GST-J^{aux} (GST–J) for 15 min at 37°C under the indicated nucleotide conditions. The "Total" lanes show the total amount of J-domain fusion protein and hsc70 loaded onto the glutathione-Sepharose beads. (D) Hsc70 R447H exhibits weak in vitro CCV uncoating activity. Clathrin released from purified CCVs incubated with either wt (squares) or mutant (diamonds) Hsc70 was determined as described in the Materials and methods. The error bars represent the standard deviation (n = 3).
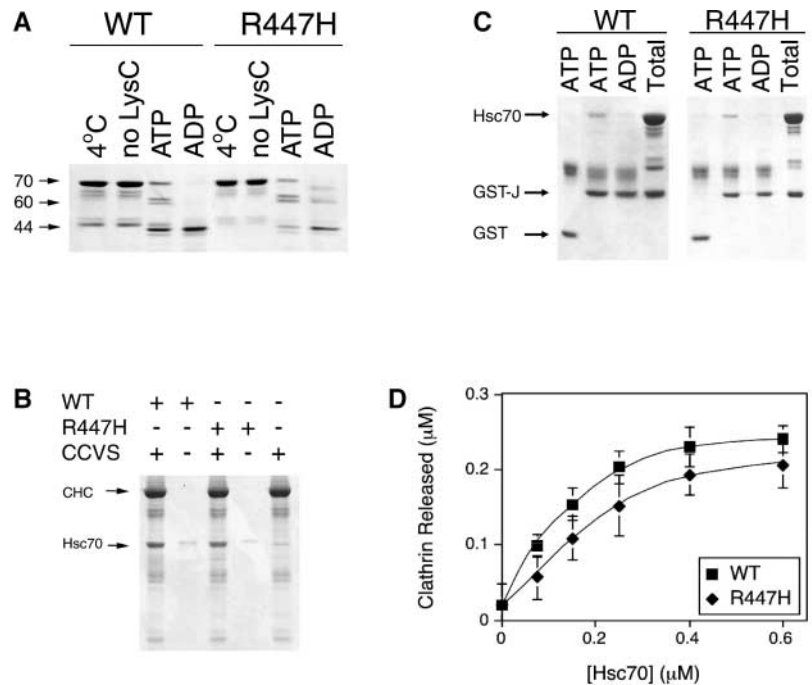
type and mutant Hsc70 to release clathrin from CCVs at increasing concentrations of Hsc70. Although the mutant protein was capable of uncoating activity, the extent of clathrin release was reduced by ~33%, and half-maximal release required 1.5–2-fold more mutant than wild-type protein (Fig. 6 D). Although the reduction was partial, in fact the extent of inhibition was in good agreement with data obtained from expressing a dominant-negative Hsc70 in HeLa cells. Expressed in the presence of excess endogenous wild-type Hsc70, a 30% reduction in uncoating activity was found to be sufficient to block transferrin receptor endocytosis and recycling. Further reductions of Hsc70 activities were shown to cause deleterious effects to cells (Newmyer and Schmid, 2001).

Discussion

We have isolated a mutant allele of *Hsc70-4* based on its phenotypic defects in Boss internalization. To understand the basis of this defect, we showed that normal function of *Hsc70-4* was required only in the Sev-expressing cells that actually mediate Boss endocytosis. Furthermore, we showed that the plasma membrane localization and functioning (cell fate specification) of the Sev receptors were not affected by this mutation, suggesting that the defect most likely occurred in the endocytic pathway. A generalized defect in endocytosis was further supported by the inhibition of uptake of a nonspecific endocytic tracer and the disruption of clathrin trafficking within Garland cells expressing the mutant allele. Moreover, the mutant allele interacted genetically with dynamin. Our data are consistent with the results of disrupting *auxilin* functions in *Caenorhabditis elegans* and *Saccharomyces cerevisiae*, in which defects in receptor-mediated endocytosis, clathrin exchange, and proper cargo delivery were observed (Pishvaee et al., 2000; Greener et al., 2001). Together, these data strongly support a physiological role for the Hsc70/auxilin system in endocytosis.

Although only one *Hsc70* allele was isolated, two lines of evidence suggested that impaired Hsc70 function was responsible for the phenotypes associated with the R447H substitution. First, the lethality and the phenotype of *Hsc70-4^{R447H}* were completely rescued by a wild-type *Hsc70-4* transgene, suggesting that it is a simple loss of function allele. Second, although we were unable to examine the Boss internalization phenotype in *FLP/FRT*-induced mutant clones using existing *Hsc70-4*–null alleles (Bronk et al., 2001), these alleles did exhibit interaction with *GMR-shi^{K39A}* (unpublished data), albeit to a weaker extent than *Hsc70-4^{R447H}*. Hsc70 is thought to function stoichiometrically in clathrin uncoating; thus, the presence of an equimolar level of mutant Hsc70 proteins might hinder the reaction more than a complete removal of one *Hsc70* locus.

Importantly, the R447H substitution was found to inhibit the extent of clathrin uncoating in vitro. Although the degree of inhibition appeared modest, it was consistent with expectations. First, because null alleles of *Hsc70-4* are cell lethal, it is highly likely that some residual activity must be maintained in order to propagate clones expressing the mutant gene. Second, transferrin endocytosis and recycling were markedly inhibited in HeLa cells overexpressing a dominant negative (ATPase deficient) Hsc70, even though the expression levels obtained corresponded to those that reduced in vitro uncoating activity by only 30% (Newmyer and Schmid, 2001). Thus, as we found for the *Hsc70-4^{R447H}* mutant, a modest reduction in uncoating activity measured in vitro was nevertheless sufficient to correlate with a dramatic reduction in endocytosis in vivo.

Although our experiments provide genetic proof of a role for Hsc70 in endocytosis, some important questions still remain. The link between uncoating as measured in vitro with the block in endocytosis observed in vivo must remain somewhat correlative because it is not possible to directly measure clathrin uncoating activity per se in intact cells. It is

highly likely, however, that the impaired uncoating activity of Hsc70^{R447H} in vitro reflects a defect in the enzyme's role in regulating clathrin function within the cell. This conclusion was strongly supported by the observed genetic interaction between *Hsc70-4* and dynamin and the profound effects of Hsc70-4^{R447H} on clathrin distribution in cells. Hsc70 is known to bind to the soluble pool of clathrin, and Hsc70–clathrin complexes are defective in self-assembly (Schlossman et al., 1984). Thus, in addition to its role in clathrin disassembly, Hsc70 may function as a chaperone to stabilize and/or maintain the function of the soluble pool of clathrin. Indeed, the nearly complete loss of identifiable CCVs and/or clathrin-coated pits in Garland cells expressing the mutant *Hsc70-4* allele is also consistent with a severe disruption in the regulation of clathrin assembly/disassembly in these mutant cells. Regardless, our observations provide strong evidence for a physiological role for Hsc70 in clathrin-mediated endocytosis.

Recent work has suggested that Hsc70 may function not just at the internalization step, but at multiple steps of the endocytic pathway, including receptor recycling (Newmyer and Schmid, 2001). Conceivably, this situation reflects a role for clathrin in recycling from endosomes, a possibility consistent with persistent observations of clathrin-coated buds apparently emanating from endosomal tubules (Stoorvogel et al., 1996; Futter et al., 1998). In addition, in polarized epithelial cells, the AP-1B clathrin adaptor complex plays a role in ensuring basolateral recycling during endocytosis (Folsch et al., 1999, 2001). On the other hand, it is possible that Hsc70 has other functions in addition to clathrin uncoating. We showed that Hk staining was disrupted in *Hsc70* mutant cells, suggesting that *Hsc70* may have a role in properly organizing endosomal compartments, although it is not yet clear how the Hk protein itself is associated with membranes. Furthermore, a novel J-domain protein, Rme8, has recently been shown to participate in endocytosis in *C. elegans* (Zhang et al., 2001). Although there is no evidence documenting direct interaction between Rme8 and Hsc70, the identification of another J-protein in the endocytic pathway certainly raises the possibility that the mechanism of Hsc70 function in endocytosis might be more complicated than previously envisioned. With the continued development of stage-specific assays for individual events during endocytic and biosynthetic membrane traffic in *Drosophila* cells, the availability of an *Hsc70-4* mutant with endocytic phenotypes will prove useful in elucidating the nature of the steps under its direct or indirect control.

Materials and methods

Fly genetics
All fly crosses were performed at 25°C in standard laboratory conditions. For the *HRP–Boss* screen, *w; FRT82^{neo}* males treated with 25 mM ethyl methanesulfonate (M0880; Sigma-Aldrich) were mass mated with *w/w; TM3, Sb/ TM6B, Hu, Tb* virgins. Individual progeny were backcrossed to *w; TM3, Sb/ TM6B, Hu, Tb* flies to establish lines. Several *w; FRT82^{neo}, mutant/TM6B, Hu, Tb* males from each line were then mated to *ey-FLP; P{w$^+$, HRP-Boss}; FRT82^{neo}, arm-lacZ* females. Eye discs were dissected from *Tb$^+$* third instar larval progeny and stained for HRP and β-galactosidase activities.

Mitotic clones in adult retina were generated using *hs-FLP1; FRT^{neo}82B, P{w+}96A* (Xu and Rubin, 1993). Mitotic clones in larval eye discs were generated using *ey-FLP; FRT82^{neo}, GMR-myrGFP-3R* (see below). To facili-

tate exogenous protein expression in larval Garland cells, UAS-derived transgenes (*UAS-GFP–rab7* and *UAS-GFP–Clc*) were driven with *Act5C-GAL4* lines.

UAS-myc::Hsc70-C1 and alleles of *Hsc70-4* were obtained from Spyros Artavanis-Tsakonas (Massachusetts General Hospital/Harvard Medical School, Boston, MA). *HRP-Boss* flies were obtained from Helmut Kramer (University of Texas Southwestern, Dallas, TX). *UAS-GFP–rab7* flies were obtained from Marcos A. González-Gaitán (Max-Planck Institute, Dresden, Germany). *Act5C-GAL4* (No. 4414), *Sev-GAL4* (No. 5793), and *sca-GAL4$^{109-68}$* (No. 6479) were obtained from the Bloomington *Drosophila* stock center (Bloomington, IN).

Histology and immunohistochemistry
For the visualization of HRP–Boss in mutant clones, eye discs dissected from third instar larvae were stained in PBS containing 0.5 mg/ml DAB and 0.003% H_2O_2 for 30 min at room temperature. The discs were then washed twice with PBS, and fixed in 2% glutaraldehyde/PBS for 40 min at 4°C. After two washes with PBS, the discs were stained for β-galactosidase activities and mounted as previously described (Wolff, 2000).

For the endocytic tracer uptake assay, dissected Garland cells were incubated with M3 complete media containing 0.2 mg/ml TR-avidin (Molecular Probes) for 1 min at 25°C. The cells were then washed with PBS, chased, and fixed with 4% paraformaldehyde/PBS for 20 min at 4°C.

Immunostaining of eye discs and Garland cells was performed according to Wolff (2000). Rabbit polyclonal αHk antibody was used at 1:500 dilution (Kramer and Phistry, 1996), mouse monoclonal αSev antibody was used at 1:10 dilution (Tomlinson et al., 1987), rat αElav antibody (Developmental Studies Hybridoma Bank, Iowa City, Iowa) was used at 1:10 dilution, rabbit αMyc antibody (Santa Cruz Biotechnology, Inc.) was used at 1:100 dilution, and mouse monoclonal α-Arm antibody (Developmental Studies Hybridoma Bank) was used at 1:10 dilution.

EM
For EM analysis, dissected Garland cells were incubated with PBS containing 0.7% HRP type VI (Sigma-Aldrich) for 5 min at 25°C. The cells were then washed with PBS and fixed with 2% paraformaldehyde/2% glutaraldehyde/PBS for 2 h at 4°C. The cells were washed repeatedly with PBS, and stained in PBS containing 0.5 mg/ml DAB and 0.003% H_2O_2 for 30 min at room temperature. The cells were then washed with PBS and postfixed with 2.5% glutaraldehyde in 0.1 M sodium cacoldylate (pH 6.8) on ice for 1 h. The cells were washed with 0.1 M sodium cacoldylate (pH 6.8), intensified in 2% OsO$_4$/0.1 M sodium cacoldylate (pH 6.8), stained with 2% uranium acetate en bloc, dehydrated with a graded ethanol series (30%, 50%, 70%, 95%, and two times 100%, 10 min each), equilibrated with two incubations (10 min) in propylene oxide, and incubated in 50% propylene oxide/50% epon resin mixture overnight. The cells were then incubated in 100% epon resin for 4 h, embedded, and baked overnight.

Scanning EM was performed according to Wolff (2000). In brief, the eyes were fixed and dehydrated through a graded ethanol series (25%, 50%, 75%, and two times 100%). The samples were then incubated in hexamethyldisilazane (Sigma-Aldrich), dried under vacuum overnight, and mounted for SEM.

DNA sequencing and molecular biology
Exons of the *Hsc70* locus were amplified from mutant genomic DNA by PCR amplification using the following primers: AGATGTCTAAAGCTCCT-GCTG and GTTTAGTCGACCTCCTCGATGG. Products from two independent PCRs were subjected to sequence analysis.

The construction of *ey-FLP; FRT82^{neo}, GMR-myrGFP* flies will be described in detail elsewhere. In brief, the first 85 amino acids of *DSrc64* (Simon et al., 1985), including the myristoylation signal, was amplified by PCR from genomic DNA and subcloned into pEGFP-N1 (CLONTECH Laboratories, Inc.) as an EcoRI-BamHI fragment. This Src–GFP fusion was then subcloned into pGMR expression vector (Hay et al., 1995) as an EcoRI-NotI fragment. To generate *GMR-shi^{K39A}*, amino acid K39(AAG) to A(GCG) change was generated by nested PCR with the following primers: GCGGATCCAAGCTTGAATTCGGACCTCGCCGCAATG, AACG-GAACTCGCGCCAGCTGA, TCAGCTGGCGCGAGTTCCGTT, and CCT-GTGGATCCACCTCC. The PCR product containing the K39A mutation was subcloned as a 600-bp BamHI fragment into pBS-dyn3 (Chen et al., 1991), and the entire *shi^{K39A}* ORF was then subcloned as an EcoRI fragment into the pGMR expression vector. To generate *UAST-GFP-Clc*, the coding region of the *Clc* gene (Vasyukevich and Bazinet, 1999) was PCR amplified from genomic DNA using the following primers: GCAAGCTTTGGACT-TCGGAGACGATTTCGC and GCTCTAGATTAGGCGAGTGCGTAAT-TAAAAC. The PCR product was subcloned into pEGFP-C1 (CLONTECH

Laboratories, Inc.) as a HindIII-XbaI fragment. The EGFP-C1-Clc fusion was then PCR amplified with GCGAATTCCACCATGGTGAGCAAGGGCG and GCTCTAGATTAGGCGAGTGCGTAATTAAAAC, and subcloned into pUAST as an EcoRI-XbaI fragment. All PCR-generated DNA constructs were verified by sequencing analysis, and the corresponding transgenic fly lines were generated by P-element–mediated transformation (Rubin and Spradling, 1982).

The pT7.7-Hsc70 construct encoding wild-type hsc70 was engineered as described previously (Newmyer and Schmid, 2001). The R447H mutation was engineered into pT7.7-Hsc70 using the QuickChange Mutagenesis Kit (Stratagene) and the following primers: GAAGGTGAGCATGCCATGAC-CAAGG and CCTTGGTCATGGCATGCTCACCTTC. The construct encoding bovine auxilin, 1034, was provided by E. Ungewickell (University of Hannover, Hannover, Germany). pGEXaux$_{813-910}$ was generated through BamHI digestion of 1034 followed by treatment with Klenow enzyme, and digestion of the isolated linearized DNA with XhoI. The resulting DNA fragment was ligated into XhoI/SmaI-digested pGEX4T-1. Verification of the engineered plasmids was confirmed through DNA sequencing.

Protein purification
CCVs were purified from fresh bovine brain as described previously (Hannan et al., 1998), and the protein concentration determined by Coomassie protein assay (Pierce Chemical Co.). The recombinant R447H Hsc70 mutant was purified similarly to the wild-type protein as previously reported (Newmyer and Schmid, 2001). GST-J^{aux} was expressed from pGEXaux$_{813-910}$ and purified on glutathione-Sepharose (Amersham Biosciences) according to the manufacturer.

Limited proteolysis
Hsc70 proteins were dialyzed against 20 mM Hepes, pH 7, 75 mM KCl, 10 mM (NH$_4$)$_2$SO$_4$, and 2 mM MgCl$_2$ to remove residual PMSF remaining from purification. Hsc70 (1 μg) was combined with 2 mM nucleotide in 10 μl 25 mM Tris, pH 8.5, 1 mM EDTA. Endoproteinase LysC (100 ng) digestion was performed at 37°C for 1 h, terminated by boiling in SDS sample buffer for 3 min, and analyzed by SDS-PAGE and staining with Coomassie blue.

Binding of Hsc70 to isolated CCVs
Hsc70 proteins (1 μM) were incubated at 25°C for 15 min with and without CCVs (9 μg) in 30 μl 100 mM Mes, pH 6.2, 1 mM EDTA, and 0.5 mM MgCl$_2$. Reactions were placed on ice and then centrifuged at 100,000 g for 10 min. A third of the isolated pellet was analyzed by SDS-PAGE, visualized with Coomassie blue staining, and quantified by densitometric methods.

Auxilin J-domain pull downs
In a total volume of 20 μl, GST-J^{aux} (4 μM) was incubated for 15 min at 25°C with 4 μM hsc70 protein and 2 mM nucleotide in uncoating buffer containing 0.1% ovalbumin and 125 mM KCl. The binding reaction was transferred to 4°C and incubated with 20 μl of GSH-Sepharose (50% slurry) with shaking for 30 min. The beads were collected by centrifugation at 16,000 g and washed twice with ice cold buffer containing the appropriate nucleotide (0.1 mM). One tenth of the bound material was analyzed by SDS-PAGE.

Clathrin release assay
Hsc70-mediated clathrin release was performed at 25°C in uncoating buffer (20 mM Hepes, pH 7, 25 mM KCl, 10 mM [NH$_4$]$_2$SO$_4$, and 2 mM MgCl$_2$) supplemented with 2 mM ATP. CCVs (4 μg in a final volume of 30 μl) were added to initiate the reaction, which was incubated for 8 min at 25°C, at which point uncoating mediated by hsc70$_{WT}$ was complete. The uncoating reaction was stopped on ice and centrifuged at 100,000 g for 10 min. The resulting supernatant was analyzed by SDS-PAGE and densitometric scanning of Coomassie blue–stained gels. The extent of clathrin release was determined by comparison to a standard curve of clathrin. Background clathrin release observed in the absence of hsc70 was subtracted from the values obtained above, yielding hsc70-dependent uncoating activity.

References

Brand, A.H., and N. Perrimon. 1993. Targeted gene expression as a means of altering cell fates and generating dominant phenotypes. *Development.* 118:401–415.

Bronk, P., J.J. Wenniger, K. Dawson-Scully, X. Guo, S. Hong, H.L. Atwood, and K.E. Zinsmaier. 2001. *Drosophila* Hsc70-4 is critical for neurotransmitter exocytosis in vivo. *Neuron.* 30:475–488.

Bukau, B., and A.L. Horwich. 1998. The Hsp70 and Hsp60 chaperone machines. *Cell.* 92:351–366.

Cagan, R.L., H. Kramer, A.C. Hart, and S.L. Zipursky. 1992. The bride of sevenless and sevenless interaction: internalization of a transmembrane ligand. *Cell.* 69:393–399.

Chappell, T.G., W.J. Welch, D.M. Schlossman, K.B. Palter, M.J. Schlesinger, and J.E. Rothman. 1986. Uncoating ATPase is a member of the 70 kilodalton family of stress proteins. *Cell.* 45:3–13.

Chappell, T.G., B.B. Konforti, S.L. Schmid, and J.E. Rothman. 1987. The ATPase core of a clathrin uncoating protein. *J. Biol. Chem.* 262:746–751.

Chen, M.S., R.A. Obar, C.C. Schroeder, T.W. Austin, C.A. Poodry, S.C. Wadsworth, and R.B. Vallee. 1991. Multiple forms of dynamin are encoded by shibire, a *Drosophila* gene involved in endocytosis. *Nature.* 351:583–586.

Damke, H., T. Baba, A.M. van der Bliek, and S.L. Schmid. 1995. Clathrin-independent pinocytosis is induced in cells overexpressing a temperature-sensitive mutant of dynamin. *J. Cell Biol.* 131:69–80.

Damke, H., D.D. Binns, H. Ueda, S.L. Schmid, and T. Baba. 2001. Dynamin GTPase domain mutants block endocytic vesicle formation at morphologically distinct stages. *Mol. Biol. Cell.* 12:2578–2589.

Entchev, E.V., A. Schwabedissen, and M. Gonzalez-Gaitan. 2000. Gradient formation of the TGF-β homolog Dpp. *Cell.* 103:981–991.

Fergestad, T., W.S. Davis, and K. Broadie. 1999. The stoned proteins regulate synaptic vesicle recycling in the presynaptic terminal. *J. Neurosci.* 19:5847–5860.

Folsch, H., H. Ohno, J.S. Bonifacino, and I. Mellman. 1999. A novel clathrin adaptor complex mediates basolateral targeting in polarized epithelial cells. *Cell.* 99:189–198.

Folsch, H., M. Pypaert, P. Schu, and I. Mellman. 2001. Distribution and function of AP-1 clathrin adaptor complexes in polarized epithelial cells. *J. Cell Biol.* 152:595–606.

Futter, C.E., A. Gibson, E.H. Allchin, S. Maxwell, L.J. Ruddock, G. Odorizzi, D. Domingo, I.S. Trowbridge, and C.R. Hopkins. 1998. In polarized MDCK cells basolateral vesicles arise from clathrin-γ-adaptin–coated domains on endosomal tubules. *J. Cell Biol.* 141:611–623.

Gaidarov, I., F. Santini, R.A. Warren, and J.H. Keen. 1999. Spatial control of coated-pit dynamics in living cells. *Nat. Cell Biol.* 1:1–7.

Greener, T., B. Grant, Y. Zhang, X. Wu, L.E. Greene, D. Hirsh, and E. Eisenberg. 2001. *Caenorhabditis elegans* auxilin: a J-domain protein essential for clathrin-mediated endocytosis in vivo. *Nat. Cell Biol.* 3:215–219.

Hannan, L.A., S.L. Newmyer, and S.L. Schmid. 1998. ATP- and cytosol-dependent release of adaptor proteins from clathrin-coated vesicles: A dual role for Hsc70. *Mol. Biol. Cell.* 9:2217–2229.

Hart, A.C., H. Kramer, D.L. Van Vactor, Jr., M. Paidhungat, and S.L. Zipursky. 1990. Induction of cell fate in the *Drosophila* retina: the bride of sevenless protein is predicted to contain a large extracellular domain and seven transmembrane segments. *Genes Dev.* 4:1835–1847.

Hay, B.A., T. Wolff, and G.M. Rubin. 1994. Expression of baculovirus P35 prevents cell death in *Drosophila*. *Development.* 120:2121–2129.

Hay, B.A., D.A. Wassarman, and G.M. Rubin. 1995. *Drosophila* homologs of baculovirus inhibitor of apoptosis proteins function to block cell death. *Cell.* 83:1253–1262.

Hing, H.K., L. Bangalore, X. Sun, and S. Artavanis-Tsakonas. 1999. Mutations in the heatshock cognate 70 protein (hsc4) modulate Notch signaling. *Eur. J. Cell Biol.* 78:690–697.

Hinshaw, J.E. 2000. Dynamin and its role in membrane fission. *Annu. Rev. Cell Dev. Biol.* 16:483–519.

Holstein, S.E., H. Ungewickell, and E. Ungewickell. 1996. Mechanism of clathrin basket dissociation: separate functions of protein domains of the DnaJ homologue auxilin. *J. Cell Biol.* 135:925–937.

Honing, S., G. Kreimer, H. Robenek, and B.M. Jockusch. 1994. Receptor-mediated endocytosis is sensitive to antibodies against the uncoating ATPase (hsc70). *J. Cell Sci.* 107:1185–1196.

Kornfeld, S., and I. Mellman. 1989. The biogenesis of lysosomes. *Annu. Rev. Cell Biol.* 5:483–525.

Kosaka, T., and K. Ikeda. 1983. Reversible blockage of membrane retrieval and endocytosis in the garland cell of the temperature-sensitive mutant of *Drosophila melanogaster*, shibire*ts1*. *J. Cell Biol.* 97:499–507.

Kramer, H., and M. Phistry. 1996. Mutations in the *Drosophila* hook gene inhibit endocytosis of the boss transmembrane ligand into multivesicular bodies. *J. Cell Biol.* 133:1205–1215.

Mayer, M.P., T. Laufen, K. Paal, J.S. McCarty, and B. Bukau. 1999. Investigation of the interaction between DnaK and DnaJ by surface plasmon resonance spectroscopy. *J. Mol. Biol.* 289:1131–1144.

Meyer, C., D. Zizioli, S. Lausmann, E.L. Eskelinen, J. Hamann, P. Saftig, K. von Figura, and P. Schu. 2000. μ1A-adaptin-deficient mice: lethality, loss of AP-1 binding and rerouting of mannose 6-phosphate receptors. *EMBO J.* 19:2193–2203.

Morgan, J.R., K. Prasad, S. Jin, G.J. Augustine, and E.M. Lafer. 2001. Uncoating of clathrin-coated vesicles in presynaptic terminals: roles for Hsc70 and auxilin. *Neuron.* 32:289–300.

Morshauser, R.C., W. Hu, H. Wang, Y. Pang, G.C. Flynn, and E.R. Zuiderweg. 1999. High-resolution solution structure of the 18 kDa substrate-binding domain of the mammalian chaperone protein Hsc70. *J. Mol. Biol.* 289:1387–1403.

Newmyer, S.L., and S.L. Schmid. 2001. Dominant-interfering Hsc70 mutants disrupt multiple stages of the clathrin-coated vesicle cycle in vivo. *J. Cell Biol.* 152:607–620.

Peifer, M., and E. Wieschaus. 1990. The segment polarity gene armadillo encodes a functionally modular protein that is the *Drosophila* homolog of human plakoglobin. *Cell.* 63:1167–1176.

Perkins, L.A., J.S. Doctor, K. Zhang, L. Stinson, N. Perrimon, and E.A. Craig. 1990. Molecular and developmental characterization of the heat shock cognate 4 gene of *Drosophila melanogaster*. *Mol. Cell. Biol.* 10:3232–3238.

Pishvaee, B., G. Costaguta, B.G. Yeung, S. Ryazantsev, T. Greener, L.E. Greene, E. Eisenberg, J.M. McCaffery, and G.S. Payne. 2000. A yeast DNA J protein required for uncoating of clathrin-coated vesicles in vivo. *Nat. Cell Biol.* 2:958–963.

Puertollano, R., R.C. Aguilar, I. Gorshkova, R.J. Crouch, and J.S. Bonifacino. 2001. Sorting of mannose 6-phosphate receptors mediated by the GGAs. *Science.* 292:1712–1716.

Richardson, H., L.V. O'Keefe, T. Marty, and R. Saint. 1995. Ectopic cyclin E expression induces premature entry into S phase and disrupts pattern formation in the *Drosophila* eye imaginal disc. *Development.* 121:3371–3379.

Robinow, S., and K. White. 1988. The locus elav of *Drosophila melanogaster* is expressed in neurons at all developmental stages. *Dev. Biol.* 126:294–303.

Rubin, G.M., and A.C. Spradling. 1982. Genetic transformation of *Drosophila* with transposable element vectors. *Science.* 218:348–353.

Schlossman, D.M., S.L. Schmid, W.A. Braell, and J.E. Rothman. 1984. An enzyme that removes clathrin coats: purification of an uncoating ATPase. *J. Cell Biol.* 99:723–733.

Schulze-Lohoff, E., A. Hasilik, and K. von Figura. 1985. Cathepsin D precursors in clathrin-coated organelles from human fibroblasts. *J. Cell Biol.* 101:824–829.

Sever, S., H. Damke, and S.L. Schmid. 2000. Garrotes, springs, ratchets, and whips: putting dynamin models to the test. *Traffic.* 1:385–392.

Simon, M.A., B. Drees, T. Kornberg, and J.M. Bishop. 1985. The nucleotide sequence and the tissue-specific expression of *Drosophila* c-src. *Cell.* 42:831–840.

Stoorvogel, W., V. Oorschot, and H.J. Geuze. 1996. A novel class of clathrin-coated vesicles budding from endosomes. *J. Cell Biol.* 132:21–33.

Sunio, A., A.B. Metcalf, and H. Kramer. 1999. Genetic dissection of endocytic trafficking in *Drosophila* using a horseradish peroxidase-bride of sevenless chimera: hook is required for normal maturation of multivesicular endosomes. *Mol. Biol. Cell.* 10:847–859.

Tomlinson, A., D.D. Bowtell, E. Hafen, and G.M. Rubin. 1987. Localization of the sevenless protein, a putative receptor for positional information, in the eye imaginal disc of *Drosophila*. *Cell.* 51:143–150.

Umeda, A., A. Meyerholz, and E. Ungewickell. 2000. Identification of the universal cofactor (auxilin 2) in clathrin coat dissociation. *Eur. J. Cell Biol.* 79:336–342.

Ungewickell, E., H. Ungewickell, S.E. Holstein, R. Lindner, K. Prasad, W. Barouch, B. Martin, L.E. Greene, and E. Eisenberg. 1995. Role of auxilin in uncoating clathrin-coated vesicles. *Nature.* 378:632–635.

van der Bliek, A.M., and E.M. Meyerowitz. 1991. Dynamin-like protein encoded by the *Drosophila* shibire gene associated with vesicular traffic. *Nature.* 351:411–414.

Vasyukevich, K., and C. Bazinet. 1999. A *Drosophila* clathrin light-chain gene: sequence, mapping, and absence of neuronal specialization. *DNA Cell Biol.* 18:235–241.

White, N.M., and A.P. Jarman. 2000. *Drosophila* atonal controls photoreceptor R8-specific properties and modulates both receptor tyrosine kinase and Hedgehog signalling. *Development.* 127:1681–1689.

Wolff, T. 2000. Histological techniques for the *Drosophila* eye. Parts I and II. *In* Drosophila Protocols. W. Sullivan, M. Ashburner, and R.S. Hawley, editors. Cold Spring Harbor Laboratory Press, Cold Spring Harbor, NY. 201–244.

Xu, T., and G.M. Rubin. 1993. Analysis of genetic mosaics in developing and adult *Drosophila* tissues. *Development.* 117:1223–1237.

Zhang, Y., B. Grant, and D. Hirsh. 2001. RME-8, a conserved J-domain protein, is required for endocytosis in *Caenorhabditis elegans*. *Mol. Biol. Cell.* 12:2011–2021.

Zipursky, S.L., and G.M. Rubin. 1994. Determination of neuronal cell fate: lessons from the R7 neuron of *Drosophila*. *Annu. Rev. Neurosci.* 17:373–397.